

**DENSITY FUNCTIONAL THEORY STUDY OF  
ELECTRONIC STRUCTURE AND MUON  
HYPERFINE INTERACTION IN GUANINE-  
CYTOSINE DOUBLE STRAND DNA MOLECULE**

**AMMAINA BINTI JAMALUDIN**

**UNIVERSITI SAINS MALAYSIA**

**2023**

**DENSITY FUNCTIONAL THEORY STUDY OF  
ELECTRONIC STRUCTURE AND MUON  
HYPERFINE INTERACTION IN GUANINE-  
CYTOSINE DOUBLE STRAND DNA MOLECULE**

by

**AMMAINA BINTI JAMALUDIN**

**Thesis submitted in fulfilment of the requirements  
for the degree of  
Doctor of Philosophy**

**December 2023**

## ACKNOWLEDGEMENT

I would like to express my gratitude to Allah SWT for giving me the opportunity and helping me endlessly in finishing this thesis. It has been a great privilege for me to be a student of Professor Dr. Shukri bin Sulaiman. I have benefited a lot from my association with him for the last 4 years. I am taking this opportunity to express my gratitude to him not only for all his guidance and help for my academic affairs, but also for his thoughts and concern in my personal life, despite his busy schedules. I would like to thank Dr. Wan Nurfadhilah binti Zaharim for being my co-supervisor, and for being patience in teaching me the quantum mechanical computational technique. In addition, I have also learned a lot from her in performing  $\mu$ SR experiments. Many thanks to Dr. Isao Watanabe who gave access to the facilities at the Advanced Centre for Computing and Communication, RIKEN. I would like to thank my laboratory mates in the Computational Physics Laboratory, School of Distance Education for all their help throughout my Ph.D study. I would like to acknowledge Ministry of Higher Education, Malaysia that has funded this research under the Newton Fund Program and Malaysia Partnership and Alliances in Research (Grant No. 203/PJJAUH/6780004) To my father, mother, sister, late brother, in-laws, niece and nephews, I have not found any word in this world that can describe my gratitude for all your love, support, encouragement, patience, and sacrifice, during my Ph.D journey. I sincerely pray to GOD that He guides and rewards all of you with the best.

## TABLE OF CONTENTS

<b>ACKNOWLEDGEMENT</b> .....	<b>ii</b>
<b>TABLE OF CONTENTS</b> .....	<b>iii</b>
<b>LIST OF TABLES</b> .....	<b>v</b>
<b>LIST OF FIGURES</b> .....	<b>vi</b>
<b>LIST OF SYMBOLS</b> .....	<b>ix</b>
<b>LIST OF ABBREVIATIONS</b> .....	<b>xi</b>
<b>LIST OF APPENDICES</b> .....	<b>xiii</b>
<b>ABSTRAK</b> .....	<b>xiv</b>
<b>ABSTRACT</b> .....	<b>xvi</b>
<b>CHAPTER 1 INTRODUCTION</b> .....	<b>1</b>
1.1 Research background .....	1
1.2 Problem statement .....	3
1.3 Objectives.....	4
1.4 Scope of study .....	4
1.5 Thesis outline .....	5
<b>CHAPTER 2 LITERATURE REVIEW</b> .....	<b>6</b>
2.1 Deoxyribonucleic acid.....	6
2.1.1 Nitrogenous bases .....	6
2.1.2 Sugar phosphate backbone .....	8
2.1.3 DNA methylation .....	9
2.2 Muon .....	9
2.2.1 Production of muon.....	10
2.2.2 Muonium .....	11
2.3 Muon Spin Rotation/ Relaxation/ Resonance .....	12
2.4 $\mu$ SR experiment study on DNA molecule.....	14

2.5	Density Functional Theory .....	16
2.6	Functional and basis sets .....	17
2.7	Computational investigation on DNA molecule .....	18
2.8	Fermi contact hyperfine interaction .....	19
<b>CHAPTER 3 METHODOLOGY.....</b>		<b>22</b>
3.1	Construction of initial geometry .....	23
3.2	Geometry optimization calculation .....	23
3.3	System of interest .....	24
3.3.1	Host system .....	25
3.3.2	Muoniated system .....	26
<b>CHAPTER 4 RESULT AND DISCUSSION.....</b>		<b>27</b>
4.1	Host system .....	27
4.1.1	Optimized structure .....	27
4.1.2	Atomic charge .....	29
4.1.3	Molecular Electrostatic Potential .....	32
4.1.4	Frontier Molecular Orbital .....	35
4.2	Muoniated system .....	43
4.2.1	Muonium trapping sites.....	43
<b>CHAPTER 5 CONCLUSION AND FUTURE RECOMMENDATIONS.....</b>		<b>55</b>
5.1	Conclusion.....	55
5.2	Recommendations for Future Research .....	57
<b>REFERENCES.....</b>		<b>59</b>

## **APPENDICES**

### **LIST OF PUBLICATIONS**

## LIST OF TABLES

	<b>Page</b>
Table 4.1	Possible Mu sites arranged in the order of increasing energy for the 1 base pair of muoniated host systems. the relative energy is taken with respect to the possible Mu trapping sites that has the minimum total energy.....44
Table 4.2	Possible Mu sites arranged in the order of increasing energy for the 2 base pair of muoniated host systems. the relative energy is taken with respect to the possible Mu trapping sites that has the minimum total energy.....45
Table 4.3	Possible Mu sites arranged in the order of increasing energy for the 3 base pair of muoniated host systems. the relative energy is taken with respect to the possible Mu trapping sites that has the minimum total energy.....48

## LIST OF FIGURES

		<b>Page</b>
Figure 2.1	Schematic of a single nucleotide arrangement.....	7
Figure 2.2	General structure of the four DNA nitrogenous bases. ....	7
Figure 2.3	Alternating chain of a sugar phosphate group in DNA.....	8
Figure 3.1	Flow chart of the methodology .....	22
Figure 4.1	Shapes and lengths of (a) ds(GC), (b) ds(GC-CG), and (c) ds(GC-CG-GC). The red lines (i) represent the lengths while the dotted lines represent the distances of O6–N4, N1–N3, and N2–O2. The green and blue lines (ii) of the figure represent the widths and distances between base stacking, respectively. ....	27
Figure 4.2	Shapes and lengths of (a) me-ds(GC), (b) me-ds(GC-CG), and (c) me-ds(GC-CG-GC). The red lines (i) represent the lengths while the dotted lines represent the distances of O6–N4, N1–N3, and N2–O2. The green and blue lines (ii) of the figure represent the widths and distances between base stacking, respectively. ....	28
Figure 4.3	Atomic charge of ds(GC) and me-ds(GC) optimized structures.....	30
Figure 4.4	Atomic charge of ds(GC-CG) and me-ds(GC-CG) optimized structures .....	30
Figure 4.5	Atomic charge of ds(GC-CGC) and me-ds(GC-CG-GC) optimized structures .....	31
Figure 4.6	Maps of molecular electrostatic potential for (a) ds(GC), (b) ds(GC- CG), and (c) ds(GC-CG- GC). The isovalue of the electron density in the maps is .....	33
Figure 4.7	Maps of molecular electrostatic potential for (a) me-ds(GC), (b) me-ds(GC- CG), and (c) me-ds(GC-CG- GC). The isovalue of the electron density in the maps is 0.002. Blue and red represent the most positive and negative regions of the electrostatic potential.	

	The potential values used for the maps range from -0.01 a.u. (red) to +0.01 .....	34
Figure 4.8	Frontier molecular orbital energies for the host systems. ....	35
Figure 4.9	HOMO-LUMO energy gap of the host systems. ....	36
Figure 4.10	(a) HOMO, (b) LUMO, and orbital composition for ds(GC). The isovalue used for the molecular orbital surface plot is 0.009 e-/au <sup>3</sup> . The composition of molecular orbitals on the right side of the figure was calculated using AOMix.....	37
Figure 4.11	(a) HOMO, (b) LUMO, and orbital composition for ds(GC-CG). The isovalue used for the molecular orbital surface plot is 0.009 e-/au <sup>3</sup> . The composition of molecular orbitals on the right side of the figure was calculated using AOMix.....	38
Figure 4.12	(a) HOMO, (b) LUMO, and orbital composition for ds(GC-CG-GC). The isovalue used for the molecular orbital surface plot is 0.009 e-/au <sup>3</sup> . The composition of molecular orbitals on the right side of the figure was calculated using AOMix. ....	39
Figure 4.13	(a) HOMO, (b) LUMO, and orbital composition for me-ds(GC). The isovalue used for the molecular orbital surface plot is 0.009 e-/au <sup>3</sup> . The composition of molecular orbitals on the right side of the figure was calculated using AOMix.....	40
Figure 4.14	(a) HOMO, (b) LUMO, and orbital composition for me-ds(GC-CG). The isovalue used for the molecular orbital surface plot is 0.009 e-/au <sup>3</sup> . The composition of molecular orbitals on the right side of the figure was calculated using AOMix. ....	41
Figure 4.15	(a) HOMO, (b) LUMO, and orbital composition for me-ds(GC-CG-GC). The isovalue used for the molecular orbital surface plot is 0.009 e-/au <sup>3</sup> . The composition of molecular orbitals on the right side of the figure was calculated using AOMix. ....	42
Figure 4.16	Scatter plot of relative energy and Mu HFCC of ds(GC-CG-GC) Mu trapping sites. The relative energy is taken with respect to the	

Mu trapping site that has the lowest total energy. Estimated ALC- $\mu$ SR resonance fields were calculated by considering  $|\Delta M|=1$ . .....52

Figure 4.17 Scatter plot of relative energy and Mu HFCC of me-ds(GC-CG-GC) Mu trapping sites. The relative energy is taken with respect to the Mu trapping site that has the lowest total energy. Estimated ALC- $\mu$ SR resonance fields were calculated by considering  $|\Delta M|=1$ .....53

## LIST OF SYMBOLS

$\theta$	Angle for the vector of electron position with respect to muon
$B(t)$	Backward detector count
$a_0$	Bohr radius
$A_\mu$	Calculated HFCC
$u$	Denotes the unpaired electrons
$v$	Denotes the paired spin orbital
$\mathbf{O}$	Dipole operator
$r$	Distance between the electron and muon
$e^-$	Electron
$\gamma_e$	Electron gyromagnetic ratio
$\Psi$	Electronic wavefunction
$\alpha_c$	Experimental calibration constant
$F(t)$	Forward detector count
$\mu$	Muon
$\gamma_\mu$	Muon gyromagnetic ratio
$\nu_\mu$	Muon neutrino
$\mu^-$	Negative muon
$\pi^-$	Negative pion
$\pi^0$ ,	Neutral pion
$\nu$	Neutrino
$A(t)$	Normalized asymmetry
$n$	Nucleons

$\Psi_v^\uparrow$	Orbitals of $\alpha$ electrons
$\Psi_v^\downarrow$	Orbitals of $\beta$ electrons
$\hbar$	Plank constant
$\mu^+$	Positive muon
$\pi^+$	Positive pion
$e^+$	Positron
$p$	Proton beam

## LIST OF ABBREVIATIONS

5mC	5-methylcytosine
ds(GC)	1 base pair guanine-cytosine double strand DNA
ds(GC-CG)	2 base pair guanine-cytosine double strand DNA
ds(GC-CG-GC)	3 base pair guanine-cytosine double strand DNA
me-ds(GC)	1 base pair methylated guanine-cytosine double strand DNA
me-ds(GC-CG)	2 base pair methylated guanine-cytosine double strand DNA
me-ds(GC-CG-GC)	3 base pair methylated guanine-cytosine double strand DNA
A	Adenine
(ALC- $\mu$ SR)	Avoided Level Crossing Muon Spin Resonance
ADF	Amsterdam Density Functional
B3LYP	Becke, Three-Parameter, Lee-Yang-Parr
C	Cytosine
DFT	Density Functional Theory
DNA	Deoxyribonucleic acid
G	Guanine
HF	Hartree-Fock
HFCC	Hyperfine coupling constant
HOMO	Highest occupied molecular orbital
LF- $\mu$ SR	Longitudinal muon spin relaxation
LUMO	Lowest unoccupied molecular orbital
MPC	Maassively Parallel Computer
MEP	Molecular electrostatic potential
$\mu$ SR	Muon Spin Rotation/Relaxation/Resonance

Mu	Muonium
NBO	Natural bond orbital analysis
T	Thymine
TF- $\mu$ SR	Transverse field muon spin rotation
UFF	Universal Force Field
ZF- $\mu$ SR	Zero field muon spin rotation

## LIST OF APPENDICES

APPENDIX A	THE BORN-OPPENHEIMER APPROXIMATION
APPENDIX B	THE SECOND HOHENBERG-KOHN THEOREM
APPENDIX C	THE FERMI CONTACT

**KAJIAN TEORI FUNGSIAN KETUMPATAN KE ATAS STRUKTUR  
ELEKTRONIK DAN INTERAKSI HIPERHALUS MUON DI DALAM  
GUANINA-SITOSINA DNA BEBENANG GANDA DUA**

**ABSTRAK**

Asid deoksiribonukleik (DNA) ialah molekul heliks berganda yang berfungsi sebagai medium untuk proses angkutan elektron yang cekap yang berkait rapat dengan kerosakan DNA dan pembangunan peranti berasaskan DNA. Kerumitan untuk memahami angkutan elektron dalam molekul DNA telah menarik minat para penyelidik untuk melaksanakan eksperimen *Muon Spin Resonance* ( $\mu$ SR) yang boleh memberikan maklumat mengenai topologi angkutan elektron, mobility elektron, dan pemalar gandingan sentuhan hiperhalus (HFCC) muon. Walau bagaimanapun, semua maklumat tersebut sangat sukar untuk ditafsir kerana struktur elektronik dan HFCC muon masih tidak jelas kerana kedudukan tapak perangkap muonium tidak diketahui. Oleh itu, Kaedah Teori Fungsi Ketumpatan (DFT) pada tahap B3LYP/6-31G telah digunakan untuk mengkaji struktur elektronik, tapak perangkap muonium, dan HFCC muon. Matlamat kajian ini adalah untuk menentukan struktur elektronik untuk sistem tulen dan bermetil 1, 2, dan 3 pasangan bes guanina-sitosina bebenang ganda dua DNA, dan untuk meramalkan nilai medan magnet luaran yang perlu dikenakan dalam *Avoided Level Crossing Muon Spin Resonance* (ALC- $\mu$ SR) untuk mencerap sebarang junaman resonan dalam spektra. Penambahan satu kumpulan metil pada atom C5 pada bes sitosina tidak menjejaskan saiz keseluruhan molekul DNA yang dikaji. Cas pada atom-atom juga tidak berubah di dalam sistem bermetil, kecuali cas pada atom C5 pada bes sitosina yang menunjukkan pertukaran nilai dari negatif kepada positif. Analisa potensi elektrostatik molekul menunjukkan kawasan yang paling reaktif adalah pada

cincin bes guanina dalam semua enam sistem yang dikaji: tiga sistem tulen, dan tiga sistem bermetil. Wujud variasi yang signifikan pada jurang HOMO-LUMO apabila bilangan pasangan bes bertambah dari 1 ke 3, untuk kedua-dua sistem tulen dan bermetil. 3.101, 3.962, and 2.015 eV adalah jurang HOMO-LUMO untuk sistem tulen manakala are 3.552, 4.634, and 3.302 eV adalah untuk system bermetil. Tapak perangkap muon yang paling stabil adalah pada C8 untuk semua sistem, tulen dan bermetil. HFCC untuk tapak yang paling stabil dalam kedua-dua sistem tulen dan bermetil masing-masing berada dalam julat 355.2 sehingga 378.7 MHz, dan 355.5 sehingga 400.5 MHz. Justeru, kawasan yang paling reaktif seperti yang ditunjukkan pada peta potensi elektrostatik molekul telah meramalkan dengan tepat kawasan untuk tapak perangkap muon yang stabil. Kajian ini juga meramalkan tiada pertindihan junaman-junaman resonan dalam spektrum ALC- $\mu$ SR kerana junaman-junaman tersebut dianggarkan untuk berlaku pada julat 1.3 sehingga 1.5 T. Kajian ini sangat penting kerana telah membuktikan bahawa pemetilan DNA tidak memberi kesan kepada HFCC pada tapak C8 sebagai tapak perangkap muon yang paling stabil.

**DENSITY FUNCTIONAL THEORY STUDY OF ELECTRONIC  
STRUCTURE AND MUON HYPERFINE INTERACTION IN GUANINE-  
CYTOSINE DOUBLE STRAND DNA MOLECULE**

**ABSTRACT**

Deoxyribonucleic acid (DNA) is a double helical molecule that serves as a medium for an efficient electron transport process that are closely related to DNA damage and development of DNA-based devices. The complexity of understanding the electron transport within DNA molecule has intrigued researchers to perform Muon Spin Resonance ( $\mu$ SR) experiment which can provide information regarding the topology of electron transport, electron mobility, and muon hyperfine coupling constant (HFCC). However, all the information is very difficult to be interpreted because the electronic structure and muon HFCC is still unclear due to the unknown position of muonium trapping sites. Therefore, Density Functional Theory (DFT) method at B3LYP/6-31G level was employed to study the electronic structure, muonium trapping sites and muon HFCC. The aims of this study are to determine the electronic structure of pure and methylated 1, 2, and 3 base pair guanine-cytosine double strand DNA, and to predict the external applied magnetic fields in Avoided Level Crossing Muon Spin Resonance (ALC- $\mu$ SR) measurements to observe any resonance dips in the spectrums. It was found that the addition of a methyl group at the C5 atom of the cytosine base does not affect the overall sizes of the studied DNA molecules. The charges of the atoms also do not change in the methylated systems except the charge at the C5 atom of cytosine base where it flips from a negative to a positive value. From the molecular electrostatic potential analysis, the most reactive region is at the guanine base ring for all six systems: three pure systems, and three

methylated systems. There is a significant variation in the HOMO-LUMO gap in going from 1 base pair to 3 base pair systems for both pure and methylated molecules. For pure systems, the HOMO-LUMO gap are 3.101, 3.962, and 2.015 eV, while for methylated systems are 3.552, 4.634, and 3.302 eV. The most stable muon trapping sites are at the C8 sites for all systems, pure and methylated. The muon HFCC for the most stable sites in both pure and methylated systems are ranging from 355.2 to 378.7 MHz, and 355.5 to 400.5 MHz, respectively. Thus, the most reactive region as shown by the molecular electrostatic potential surface plot correctly predicts the region for stable muon stopping sites. This study also predicts that there will be no overlaps in the resonance dips in the ALC- $\mu$ SR spectrums for all the six systems as the spectrums are estimated to occur at the range of 1.3 to 1.5 T. This study is very significant as it proves that methylation of DNA does not affect the muon HFCC at C8 site as the most possible muon trapping site.

# CHAPTER 1

## INTRODUCTION

### 1.1 Research background

Deoxyribonucleic acid (DNA) is a blueprint for all living organisms as it carries genetic code for the living organisms to develop, function, and reproduce [1]. The double helical DNA is an efficient medium for electron transports as it allows the electron to travel between the pi-stacking base pairs [2– 4]. Electron transport plays an important role in many biological processes in cells such as DNA damage repair, transcription factors and consumption of energy [3]. Topic regarding electron transport in DNA has intrigued many researchers to perform investigations both experimentally and theoretically.

DNA is crucial for the maintenance of cellular functions and genomic stability. Regardless of how crucial the DNA is, it still prone to a wide range of damage from various physical and chemical agents. DNA damage and electron transport are very well connected. The electronic structure of the DNA molecule will change depends on the type of damages. Different type of damages causes different changes in the electronic structure of the DNA molecule. The changing of the electronic configuration will alter the electron transport process within the DNA molecule. DNA damage distorts the local structure of the double helix structure which then interrupts the pi-stacking base pairs interactions. Thus, the interruptions affect the efficiency of the electron transfer process within the deoxyribonucleic acid. In order to maintain the genomic stability, there is DNA repair mechanisms which involve DNA repair enzyme. However, this repairing process itself requires electron transfer reactions which the efficiency has been affected by the damaged DNA. It is very important to

know the degree and type of alterations, but it is very difficult to investigate. This is the reason investigations at the subatomic level are needed.

In the late 1990, scientists found that DNA might function as a molecular wire as it could conduct charges over long distances. This discovery had attracted many researchers to study about the development of DNA based molecular devices such as biosensor, nanoelectronics and data storages. Current technology, using the principle of chemical processes enables the synthesis and modification of DNA molecules of any base pair sequences. This allows the synthetic DNA biopolymer to have specific electronic functionalities that meet the requirements of different applications. However, it is very expensive to produce synthetic DNA biopolymer in a bug scale. In consequence, the development of DNA based molecular devices in achieving efficient electron transport through DNA remains challenging. Therefore, to enhance their performance and stability, studies at the microscopic level are required.

Muon Spin Rotation/Relaxation/Resonance ( $\mu$ SR) is an excellent experimental method to study microscopic properties and processes of various materials including biological molecule[5– 9]. Torikai et al. (2001,2006) was the first to start using  $\mu$ SR to study the electron transport in DNA by using perfect DNA derived from the Herring's sperm [6, 7]. The samples that they used are complex and unknown in sequence, thus it is very difficult to continue their studies based on their sample. Another group of researchers, Hubbard et al. (2004) had performed muon spectroscopy on real double strand DNA molecules to investigate their muon properties. They observed many overlapping muonium (Mu) resonance signals in the Avoided Level Crossing Muon Spin Resonance (ALC- $\mu$ SR) spectrum, and this is also due to the complexity of the real DNA sample and its unknown sequence [5].

Electron transport topology, electron mobility, and muon hyperfine coupling constant (HFCC) are the three main information that can be obtained from the  $\mu$ SR measurements.  $\mu$ SR techniques is an ideal probe for internal structure since muon HFCC is highly sensitive to its local surroundings.  $\mu$ SR data interpretation needs information regarding the location of the muon trapping sites but this particular detail cannot be obtained from the experimental method. Typically, computational studies are used as part of the  $\mu$ SR data interpretation and analysis.  $\mu$ SR is an experimental technique that can be used to study electron transport phenomena in DNA at the microscopic level [10]. The muon labelling method is an excellent method to detect and study the electron transfer in DNA strands. Three important types of information can be obtained from  $\mu$ SR measurements. These include the topology of electron transport, electron mobility, and muon hyperfine coupling constant. An important aspect in the interpretation of  $\mu$ SR data is the knowledge of the muonium trapping sites in the sample which cannot be determined experimentally. The interpretation and analysis of the  $\mu$ SR results are normally complemented with computational studies [11].

## **1.2 Problem statement**

DNA that stores genetic information is now identified as a medium for the efficient electron transport process. Electron transport in DNA is close related to type of damages that occur in DNA and to the development of the DNA based devices such as molecular electronics. However, it is very difficult to understand the electron transport in DNA. Therefore, series of experimental and theoretical investigations by using full scopes of physicals and biochemical methods are triggered.  $\mu$ SR experimental technique has been successfully used to understand the electron transport

in DNA [6–8].  $\mu$ SR is used to study the diffusion rate of electron in DNA by utilising muon as a probe. In order to interpret the  $\mu$ SR's result, it is important to know the position of the muon. This is because the analysis of electron's diffusion rate requires information about the muon HFCC. Experimentally, it is extremely difficult to measure the muon HFCC in DNA samples. Therefore, application of computational method such as Density Functional Theory (DFT) is very crucial in this research. DFT produces quite accurate results for electronic structure calculations, and it is very valuable to obtain an idea about the position of the muon.

### **1.3 Objectives**

This research seeks to provide answers to the issues raised in section 1.2. There are four objectives to achieve goals of this research which are listed below.

1. To identify the effect of the number of base pair on the electronic structure of guanine-cytosine double strand DNA.
2. To investigate the effect of methylation on the HOMO-LUMO energy gap of 1, 2, and 3 base pair of guanine-cytosine double strand DNA.
3. To determine the muonium trapping sites in 1, 2, and 3 base pair of guanine-cytosine double strand DNA.
4. To determine the muon hyperfine coupling constant in 1, 2, and 3 base pair of guanine-cytosine double strand DNA.

### **1.4 Scope of study**

Guanine-cytosine double strand DNA molecule is the main focus in the computational work of this study. This study focuses on guanine-cytosine base pair because based on the previous experimental works, guanine has the lowest energy. This indicates that guanine has the most stable Mu trapping sites [5, 11, 12]. Next, 1,

2, and 3 base pair of guanine-cytosine double strand DNA were chosen to be investigated in this studied for two reasons. Firstly, all the three number of base pairs would be computationally practical to use the available supercomputers at the RIKEN's HOKUSAI supercomputing facility that was used in this research. Secondly, to understand the electronic properties of guanine- cytosine double strand DNA as the number of base pair increases.

## **1.5 Thesis outline**

There are 5 chapters in this thesis. This chapter 1 serves as the introductory chapter that provides background information about the research, problem statement, and objectives. Chapter 2 highlights relevant previous computational and experimental works. The description of the methods and procedures performed in this research are given in Chapter 3. In Chapter 4, the results of the analysis and the related discussion are reported. Lastly, Chapter 5 presents a summary and conclusions of this research, followed by the path for future studies.

## CHAPTER 2

### LITERATURE REVIEW

#### 2.1 Deoxyribonucleic acid

DNA is a complex structure made up of nucleotides that hold genetics instructions for an organism to develop, live, and reproduce. Nucleotides are composed of deoxyribose sugar group, phosphate group and nitrogenous bases that attached together to form two antiparallel polynucleotides strands. Watson-Crick discovered that the two antiparallel polynucleotides strands are twisted around each other in the form of double helix structure. DNA is the fundamental of research in large number of fields, such as human genome study, genetic engineering, nanodevices, and others.

##### 2.1.1 Nitrogenous bases

Figure 2.2 shows four types of nitrogenous bases which are Guanine (G), Adenine (A), Cytosine (C), and Thymine (T). There will be one type of nitrogenous base in each nucleotide which covalently attached to the sugar phosphate group as can be seen in Figure 2.1. The order of these bases in DNA sequence will form gene which will provide significant information for a living organism to make molecules called proteins. These nitrogenous bases can be classified into two groups: purines (A and G) and pyrimidines (C and T). Purines have a double ring structure that composed of a six- membered ring fused to a five-membered ring whereas pyrimidines consist of a single six-atoms ring [1, 13]. Both purines and pyrimidines are heterocyclic molecules because they have carbon and nitrogen, with hydrogen attached in the ring[14, 15]. G, A, C, and T are very flexible molecules and possess non-planar effective conformation [16]. The geometries of all the nitrogenous bases are spread between many conformations correspond to the minimum potential energy [16– 18].

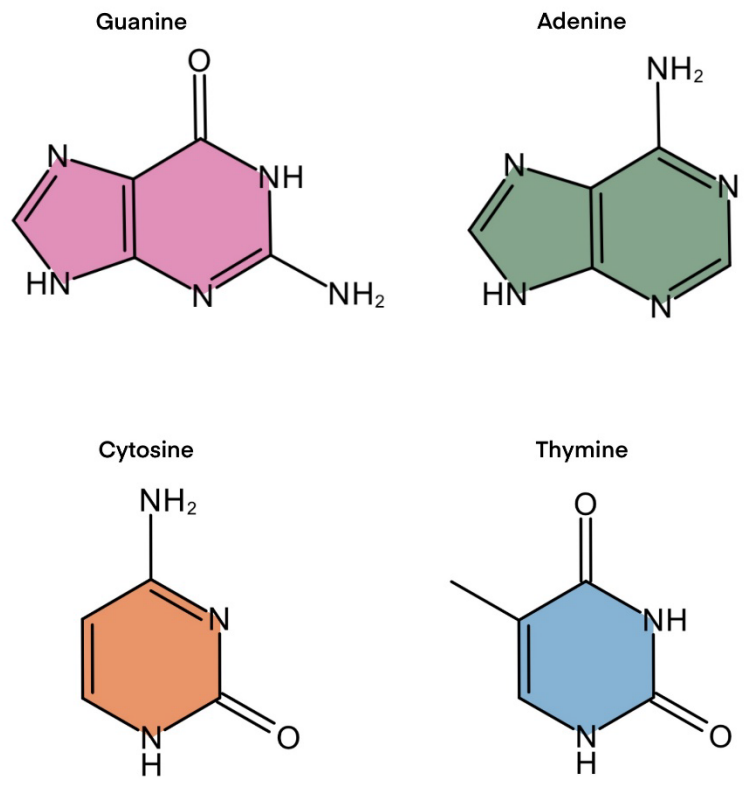


Figure 2.2 General structure of the four DNA nitrogenous bases.

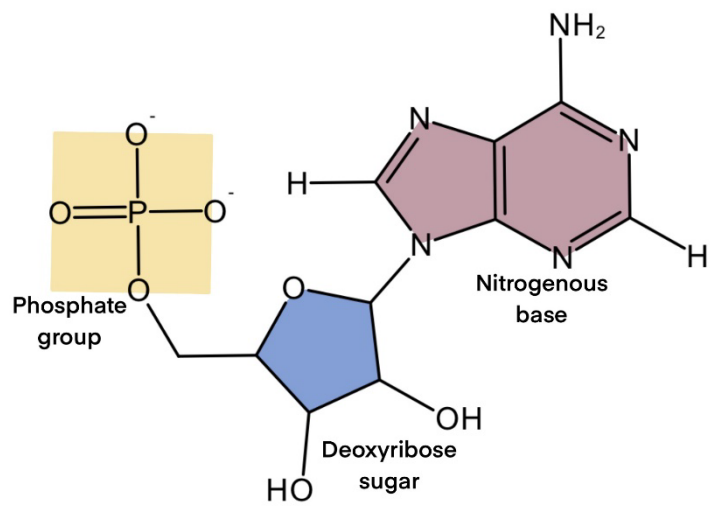


Figure 2.1 Schematic of a single nucleotide arrangement.



### 2.1.3 DNA methylation

The unrepaired DNA damages can accumulate in both replicating cells and non-replicating cells. DNA methylation is one of the unrepaired DNA damages as it changes the DNA segment activity without changing the DNA sequence. Methylation is a biological process of adding methyl group to the DNA molecule. The most common DNA methylation in human occurs largely in the distribution of CG sequence, which is 5-methylcytosine (5mC)[22]. DNA methyltransferases are an enzyme that transfer a methyl group to fifth carbon of cytosine residue to form 5mC. Methylation of DNA gives effect to the DNA structure by stabilizing the double helix structure and reducing the flexibility of the DNA. Apart from that, addition of the methyl group to the DNA also effects the interactions between DNA and proteins. The presence of methyl group in DNA blocks the transcription because the transcriptional repressor binds to the methyl group and cause the chromatin structure to increase in rigidity which leads to inefficient binding of the transcription activation factors to DNA.

## 2.2 Muon

Anderson and Neddermeyer discovered muon when they performed a cosmic radiation research in the year of 1937 [23– 25]. Muon ( $\mu$ ) is a charged elementary particle. There is muon with -1 charge,  $\mu^-$  and muon with +1 charge,  $\mu^+$  refers as antimuon. In the  $\mu$ SR scientific community,  $\mu^+$  is commonly used in the experiment and the term muon is applied to  $\mu^+$  in the literature. Primarily because  $\mu^+$  has higher production rates and the polarization is preserved during the implantation of  $\mu^+$  into the material in comparison to the negative muon due to spin-orbit coupling [26]. Consequently, the term muon that referred to  $\mu^+$  is applied throughout this thesis to

make it compatible with the literature. The muon has identical properties to the electron, but it has a mass that is 207 times greater. It also considered as a light proton with a mass of one ninth that of proton with magnetic moment 3.18334 larger [23–25].

### 2.2.1 Production of muon

Pion decay is a process that produces muon. Pion is an elementary particle of meson family, exists in three forms: positively charged ( $\pi^+$ ), negatively charged ( $\pi^-$ ) and neutrally charged ( $\pi^0$ ). The pion is an unstable particle with a lifetime of 26 ns that can be produced from high energy proton such as cosmic rays that hit other particles at the atmosphere [27]. Pion also can be produced scientifically using a particle accelerator. The accelerator will accelerate high energy proton beam ( $p$ ) with 600 MeV to 800 MeV kinetic energy which then collides with the nucleons ( $n$ ) of the production target atoms such as liquid metal target [27]. The process is characterized below:



Due to the short lifetime, pion will decay into another unstable particle, which is muon ( $\mu$ ) and muon neutrinos ( $\nu_\mu$ ). The muon is completely polarized in the centre of the mass system [27]. The pion decays process is as follows:



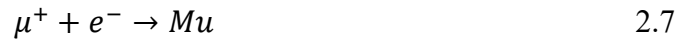
Muon has 2.197  $\mu\text{s}$  of mean lifetime which is the second longest-lived unstable subatomic particle after neutron. It will also undergo decay process as follows:



In the process 2.5 and 2.6, the positron ( $e^+$ ) and the electron ( $e^-$ ), and a pair of neutrinos ( $\nu$ ) are produced from the muon decaying process.

### 2.2.2 Muonium

After muon was discovered, researchers agree to do detail observation about an atom consisting of a positive muon ( $\mu^+$ ) and an electron [28, 29]. The positive muon, when injected into a certain material, will slow down, and capture an electron from an atom of the material. A stable atomic state called muonium (Mu) is produced [29]. The process is shown as follows:



Mu is considered as light radioisotope of hydrogen. The muon reduced mass is 0.995 that of hydrogen and which mean Mu and hydrogen have equivalent shape, size, and energy of the electron orbitals [10, 30– 35]. The Born–Oppenheimer approximation can be applied for calculations that used positive muon because muonium has essentially the same ionization potential and Bohr radius as of hydrogen [33, 34].

### 2.3 Muon Spin Rotation/ Relaxation/ Resonance

Muon spin rotation/relaxation/resonance ( $\mu$ SR) is an excellent experimental technique that has been proven excellent in studying wide range of materials in condensed matter physics and materials science fields.  $\mu$ SR measurement is a well-established method that used positive muon  $\mu^+$  to study the microscopic structures, electronic properties, and processes at the atomic scale [26, 27, 37– 39]. The positive muons that are injected into a sample are produced by a muon source. Two type of muon sources are available: pulsed source beam and continuous source beam. The pulsed source beam deliver muon in discrete pulses which usually generated using shorter width proton pulses. All muons are assumed to arrive simultaneously. In contrast, the continuous source beam allows each individual muon hitting the target to be detected on-at-a-time [26, 27, 37, 40].

$\mu$ SR experimental method can work with a variety of materials, including liquid, solid, and gas as the spectrometer is equipped with a different possible sample environments including a furnace, dilution refrigerator, helium cryostat, closed cycle refrigerator, and external magnetic field [40]. This experimental technique can be applied with several kinds of external magnetic fields depend on the purpose of the experiment. The external magnetic fields are transverse field muon spin rotation (TF- $\mu$ SR), longitudinal muon spin relaxation (LF- $\mu$ SR), and zero field muon spin relaxation (ZF- $\mu$ SR) [26, 27, 37– 39]. The external magnetic field, temperature, pressure, and radio frequency pulses are the example of sample parameters that can be selected in  $\mu$ SR measurements.

After all the parameters has been selected, a positive muon beam with a spin polarization of 100% is introduced into the material of the sample [26, 27, 38, 39]. Sample that made up from organic materials contain molecules with unsaturated bonds

like double or triple bond. Thus, for the organic material sample, the injected positive muon is drawn to the atoms having unsaturated bonds such as carbon atoms [10, 11, 26, 27, 35, 42]. This is because unsaturated bonds tend to have unpaired electrons that are more reactive than paired electrons. For example, the addition of positive muon into the atoms of the material will break the double bond and form a single covalent bond with one of the atoms. Of all the atoms having unsaturated bonds, the positive muon tends to bind with atom that have high binding energy. As a result, the positive muon is more stable when trapped at the specific atom [42].

The prepared sample is placed in the path of the muon beam. Muons that are generated by high-energy particle accelerator is directed onto the sample and implanted themselves at specific lattice sites within the sample. The implanted muons undergo spin precession around the local magnetic field direction as each of the muons have spin angular momentum. During the spin precession, the muons undergo through spin lattice relaxation process in which the muons interact with the phonons and the electronic environment of the material [43]. The muon will also decay over time during muons spin precession and releasing positrons that will be detected by forward and backward detectors. Both detectors will detect the emitted positrons that provide information about the muon spin polarization and the magnetic field components. The information is recorded as a time spectrum. The details can be deduced by comparing the positron count rate with respect to the muons initial momentum and position by using the following normalized asymmetry function [26, 27, 37, 44, 45].

$$A(t) = \frac{F(t) - \alpha_c B(t)}{F(t) + \alpha_c B(t)} \quad 2.8$$

where

$A(t)$  is the normalized asymmetry

$F(t)$  is the forward detector count

$B(t)$  is the backward detector count

$\alpha_c$  is the experimental calibration constant

The normalized asymmetry  $A(t)$  parameter is calculated using the difference between the forward positron  $F(t)$  count and the backward positron  $B(t)$  count.  $\alpha_c$  is the experimental calibration constant for both detectors' efficiencies [45]. Further analysis on the time spectrum is performed by using appropriate function such as Lorentzian function or Risch-Kiehr function [47, 48].

#### **2.4 $\mu$ SR experiment study on DNA molecule**

The  $\mu$ SR technique that were used to study rapid electron motion in Cytochrome *c* and myoglobin had paved the path for studying electron transport in DNA microscopically by using charge conductivity. Torikai et al. (2001) employed A- and B-forms DNA, which have different water molecule concentrations and base pair structural alignment along the strands [8]. The DNA samples were place at room temperature and the samples were given with 4 MeV  $\mu$  beam. The findings showed that the finite contribution of 3D electron transport to the nearby strands was implied by the low field behaviour in B-form. In contrast, the predominant motion in A-form was the quasi-1D motion along the strand [8]. The  $\mu$ SR method was successfully applied to study about electron transport in DNA, but based on Torikai et al. (2001), they require extended research to probe electron transport phenomena in DNA [8].

The sensitivity of muon spin relaxation caused by the environment may provide distinct outcomes for muon behaviour in A-form DNA and B-form DNA. Therefore, the  $\mu$ SR measurements were performed on the on A- and B-form DNA by adjusting the temperature from 160 to 353 K [6]. Nagamine et al. (2004) observed a drastic change of the  $\mu$  spin relaxation for both A- and B-form DNA in low magnetic field for the temperature below 260 K down to 200 K. The formation of Mu state was observed in both A-form and B-form DNA [6]. The results obtained were still limited for further discussions because the information about muons stopping site that emit and probe the labelled electrons were needed.

The ability of  $\mu$ SR procedure to extract more microscopic information about DNA has attracted many researchers. Hubbard et al. (2004) used longitudinal field (LF) ALC- $\mu$ SR experimental measurements and ab initio DFT calculations to study the muonium hyperfine interactions in powder samples of guanine, adenine, cytosine, and thymine nucleobases [5]. The LF ALC- $\mu$ SR method was employed on polycrystalline samples at different temperature. The result showed that the different temperature produces similar resonance field that caused polarization dips in the ALC- $\mu$ SR spectra [5]. They also performed DFT calculations by using Amsterdam Density Functional (ADF) program to compare the Mu hyperfine interactions with the  $\mu$ SR experimental outcomes. The ab initio DFT calculations were performed on single nucleobases. They then broaden their research by performing the LF ALC- $\mu$ SR experimental technique on real DNA extracted from Herring's sperm [5]. However, Hubbard et al. (2004) could not obtain the Mu hyperfine interaction data. This is because the real DNA was too complex, and the spectrum produce many overlapping polarization dips. Thus, Hubbard et al. (2004) stated that the study must be started with

simple DNA structures and the ab initio calculations must be used to follow the alterations that take place during the study [5].

In 2019, McKenzie (2019) performed ALC- $\mu$ SR experiment to characterize the radicals formed by Mu addition to adenine, guanine, cytosine, and thymine nucleobase [12]. The ALC- $\mu$ SR experiment was assigned by considering the existed literature regarding the estimated relative energies of the muoniated products and the muon hyperfine coupling constants of the corresponding hydrogenated radicals [12].

In conclusion, DNA molecules have been effectively studied using the  $\mu$ SR experimental technique. There are some details, nonetheless, that the  $\mu$ SR experimental technique cannot reveal. However, this problem can be solved by using the appropriate computational techniques.

## **2.5 Density Functional Theory**

DFT is a powerful method for analysing various systems and phenomena. This method that was published by Hohenberg & Kohn in 1964 has been successfully used to precisely describe various properties of atoms, molecules, and solids [49, 50]. A key concept in DFT is the electron density, which explains the probability distribution of electrons around atomic nuclei of a molecule [50].

Before DFT, there were few traditional quantum mechanics methods to provide mathematical descriptions about the electron density of molecular systems. The traditional methods were not feasible because the methods needed to deal with complex many-electron wavefunction and solve Schrödinger equation for each electron. In contrast, DFT simplify the complex wavefunctions by focusing on electron at a particular point in space [52, 53].

Therefore, DFT could be applied on large systems and provides very accurate results. DFT is based on the Hohenberg-Kohn theorem, which states that electron density and external potential of the quantum system are the only factors that can affect its ground-state energy. Use of DFT in real-world settings need an approximation for the exchange-correlation energy because it determines degrees of accuracy and computing efficiency of DFT [51, 52]. Therefore, there are many types of exchange-correlation functionals that have been developed.

## **2.6 Functional and basis sets**

Exchange-correlation energy is the energy that is responsible for the electron repulsion and includes complex electron-electron correlations that are difficult to precisely define. These two crucial quantum mechanical phenomena: the exchange effect, whereby electrons reject one another because they are indistinguishable, and the correlation effect, which explains the intricate relationships between electrons, are the sources of this energy.

There are many types of functionals that could be used in DFT technique [53]. One of the most used functionals is the DFT hybrid functionals because these functionals have the ability to maintain computational efficiency with increased accuracy for a variety of systems and properties [54]. Hybrids functionals combined two theoretical methods, which are DFT and Hartree-Fock (HF) theories. DFT theory offers computational efficiency and flexibility while HF theory provides more precise consideration of electron correlation effects, especially in systems with localized electrons. Popular example of DFT hybrid functionals is Becke, Three-Parameter, Lee-Yang-Parr (B3LYP). It is the combination of Becke exchange functional with the LYP

correlation functional. B3LYP provides accurate information for molecular geometries, vibrational frequencies, and reaction energies [54, 55].

Basis sets play a crucial role in DFT computations by approximating the electrons' wave functions within the system under investigation. It consists set of mathematical functions that are built around the atomic nuclei and are used to illustrate the electronic structure of the molecular system [55].

Various types of basis sets are available to be utilised in DFT calculations. One of the examples is Gaussian basis sets, which are frequently used in DFT methods. Gaussian basis sets focused on the atomic nuclei and are mathematically convenient for defining the molecular wave function. The basis sets are often identified by letters to denote the size and quality.

6-31G basis set is one of the examples that has been widely used to study molecular electronic structure by using DFT method. The 6-31G basis set includes 6 basis functions for each atom (3 "s" functions and 3 "p" functions) and incorporates polarization functions to improve accuracy in describing electron distribution. It is a relatively compact basis set that provides reasonable accuracy for a wide range of molecular calculations while being computationally tractable for larger systems.

## **2.7 Computational investigation on DNA molecule**

Exact values of Mu HFCC in DNA molecules can be given by the  $\mu$ SR measurements. However, the experimental method could not provide the location where the muon is trapped. In order to obtain the crucial information, the experimental method must be remedied by computational methods. The computational studies could provide precise Mu trapping sites within the DNA sample used. A variety of

computational studies have been conducted in the past such as Hartree-Fork (HF), and ab initio DFT [57– 59].

Scheicher et al. (2004, 2006) performed HF cluster method on isolated A- and B-form DNA and had found that the muon HFCC values are different between A- and B-form DNA [57, 59]. Zaharim et al. (2020, 2021, 2022) employed DFT calculations on different structures of DNA molecules [11, 35, 42, 60]. Different type of nitrogenous bases will have different values of muon hyperfine coupling constant. This is because each nitrogenous bases have different electronic structures which results in various local environment for Mu. Furthermore, the existence of sugar phosphate group in the DNA structures also gave impact to the muon hyperfine interaction [11, 35, 42, 60]. They found that C8 site of the guanine bases were the most stable muonium trapping sites for guanine nucleotide, guanine nucleobase, and guanine single strand DNA [11, 35, 42, 60].

## **2.8 Fermi contact hyperfine interaction**

Hyperfine interaction is a crucial physics phenomenon to understand quantum mechanics at the atomic and subatomic scale [60]. The hyperfine interaction is a magnetic interaction between the nuclear and its surrounding electronic spins [62– 64]. It is highly sensitive to the local electronic structure close to the nuclei where the interaction takes place because different electron configurations and different spin density can lead to different hyperfine interaction strengths. Generally, this interaction is substantially smaller than the energy levels of the nucleus itself because the nucleus is hold together by strong nuclear forces. Even though the hyperfine interaction is small in magnitude, it is still important because its effect can accurately provide valuable information about the material used at the microscopic level.

The Fermi contact interaction in a molecule involves the coupling between the nuclear magnetic moment and the electron spin density at the nucleus which only occurs in s orbitals [64, 65]. The following formula can be used to calculate the Fermi contact coupling constant, A [64, 66].

$$A = \frac{4}{3} \gamma_e \gamma_\mu \hbar (10^{-6} a_0^{-3}) \left[ |\Psi_u^\uparrow(R)|^2 + \sum_v \{ |\Psi_v^\uparrow(R)|^2 - |\Psi_v^\downarrow(R)|^2 \} \right] \quad 2.9$$

where

$\gamma_e$  is the electron gyromagnetic ratio

$\gamma_\mu$  is the muon gyromagnetic ratio

$\hbar$  is the plank constant

$a_0$  is the Bohr radius

$\Psi$  is the electronic wavefunction

$u$  denotes the unpaired electrons

$v$  denotes the paired spin orbital

$O$  is the dipole operator

$\Psi_v^\uparrow$  is the orbitals of  $\alpha$  electrons

$\Psi_v^\downarrow$  is the orbitals of  $\beta$  electrons

The dipole operator  $\mathbf{O}$  is

$$\mathbf{O} = \frac{3 \cos^2 \theta - 1}{r^3} \quad 2.10$$

Where

$r$  is the distance between the electron and muon

$\theta$  is the angle for the vector of electron position with respect to muon

## CHAPTER 3

### METHODOLOGY

This chapter explains various procedures that were used in collecting data and analysis which are relevant to the study. The six systems that were studied in this research are 1 base pair guanine-cytosine double strand DNA [ds(GC)], 2 base pair guanine-cytosine double strand DNA [ds(GC-CG)], 3 base pair guanine-cytosine double strand DNA [ds(GC-CG-GC)], 1 base pair methylated guanine-cytosine double strand DNA [me-ds(GC)], 2 base pair methylated guanine-cytosine double strand DNA [me-ds(GC-CG)], and 3 base pair methylated guanine-cytosine double strand DNA [me-ds(GC-CG-GC)]. All the molecules were generated by using Avogadro Software. The generated molecules were then investigated computationally using DFT to determine electronic structures and hyperfine interactions. Figure 3.1 shows the flow chart of the methods used in this study.

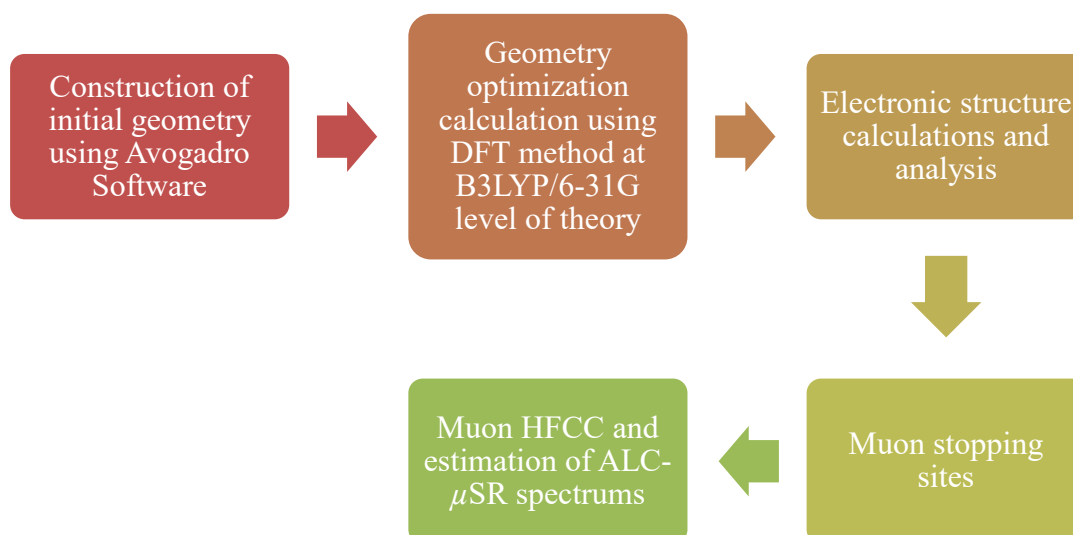


Figure 3.1 Flow chart of the methodology

### **3.1 Construction of initial geometry**

The initial geometry of the molecule was constructed using Avogadro Software [11, 35, 42, 67]. Avogadro Software was an excellent chemical builder and molecule editor that was particularly useful for visualization and analysis. It had been applied in computational chemistry, molecular modelling, bioinformatics, materials science, architecture, and other related fields [67, 68].

The initial structure of the molecule first created in Avogadro by inserting the pre-built fragments of common molecules, ligands, or amino-acid sequences. The atom-centered manipulated tool was always selected after the fragment had been inserted, making it simple to move or rotate the fragment into position. The constructed molecule was optimized using molecular mechanics that was provided by the auto-optimization tools. The force field in Avogadro was set to the default force field which is Universal Force Field (UFF). Once the optimization was completed, Gaussian 16 input coordinates were generated in Avogadro Software. The optimized geometry and the generated Gaussian 16 input coordinates were used for further optimization and calculation in the Gaussian 16 software package [68].

### **3.2 Geometry optimization calculation**

Geometry optimization was one of the initial procedures of any computational chemistry calculation in order to find stable molecular configuration with minimum energy [68, 70– 73]. All of the geometry optimization calculations were set to the default values in Gaussian 16 software package without setting symmetry limitations and performed using DFT quantum mechanical procedure at B3LYP/6-31G level [11, 35, 42, 69]. The Gaussian 16 software package is installed at the RIKEN Hokusai GreatWave Supercomputing Facility. Massively Parallel Computer (MPC) comprises

FUJITSU Supercomputer PRIMEHPC FX100 with high performance processors SPARC64 Xlfx and high perform memory systems is used [73].

The geometry optimization procedure first calculates force on each atom by evaluating the gradient (first derivative) of the energy with respect to the atomic positions before proceeds to find a new geometry with a lower energy. DFT was used at each step to select new molecule configuration, allowing the procedure to quickly converge towards the minimum energy. The optimization calculation stops when the final minimum energy geometry reaches convergence, which the root-mean-square of all the forces are zero.

This procedure provides important information regarding the spatial coordinate, optimized parameters such as bond length and bond angle, frontier molecular orbital, atomic charges and dipole moments. The new optimized structure obtained from the accomplished geometry optimization calculation is used in the following step which was population analysis.

### **3.3 System of interest**

All the optimized geometries of the molecules are used as the host systems to study the muoniated radicals. The host systems that were referred as pure and methylated systems are 1 base pair guanine-cytosine double strand DNA [ds(GC)], 2 base pair guanine-cytosine double strand DNA [ds(GC-CG)], 3 base pair guanine-cytosine double strand DNA [ds(GC-CG-GC)], 1 base pair methylated guanine-cytosine double strand DNA [me-ds(GC)], 2 base pair methylated guanine-cytosine double strand DNA [me-ds(GC-CG)], and 3 base pair methylated guanine-cytosine double strand DNA [me-ds(GC-CG-GC)]. The addition of a Mu makes each of the six